Nishina Memorial Lecture

FROM RICE TO SNOW

Pierre-Gilles de Gennes

Collège de France, 11 place M. Berthelot
75231 Paris Cedex, France

April, 1998

From rice to snow

Nishina Memorial Lecture delivered at
Department of Physics, University of Tokyo on
April 3, 1998

From rice to snow

Pierre-Gilles de Gennes

Collège de France, 11 place M. Berthelot
75231 Paris Cedex 05, France

abstract

We present here some general features of granular materials, of their importance, and of the conceptual difficulties which they exhibit. For static problems, we insist on the difference between *textures*, which represent frozen correlations between grains, and stress tensors. We argue that in systems like heaps and silos, texture is present, but the main features of the stress distribution do not depend on it, and a description using an isotropic medium is a good starting point. We also discuss avalanche flows, using a modified version of the equations of Bouchaud et al, which might be valid for thick avalanches.

1 Examples of granular matter

Solid particles are omnipresent : from the rings of Saturn to the snow of our mountains. Granular materials represent a major object of human activities : as measured in tons, the first material manipulated on earth is water ; the second is granular matter [1].

This may show up in very different forms : rice, corn, powders for construction (the elinkers which will turn into concrete), pharmaceuticals, $\cdots$. In our supposedly modern age, we are extraordinarily clumsy with granular materials. Changing the size, for instance, is difficult : crushing a granular system spends an unreasonable amount of energy, and also leads to an extremely wide distribution of sizes. Transporting a granular material is not easy : sometimes it flows like an honest fluid, but sometimes (in hoppers) it may get stuck : the reopening procedures are complicated — and often dangerous.

Even storage is a problem. The contents of bags can clump. Silos can explode, because of two features :

a) Fine powders of organic materials in air often achieve the optimum ratio of organic/ambient oxygen for detonations.

b) Most grains, when transported, acquire charge by collisions (tribo electricity) : high voltages build up, and create sparks.

From a fundamental point of view, granular systems are also very special. The general definition is based on size. We talk of particles which are large enough for thermal agitation to be negligible. Granular matter is a zero temperature system. In practice, Brownian motion may be ignored for particles *larger than one micrometer* : this is our threshold.

A heap of grains is *metastable* : ideally, on a flat horizontal support, it should spread into a monolayer (to decrease its gravitational energy). But it does not ! It can be in a variety of frozen states, and the detailed stress distribution, inside the heap, depends on sample history. (We come back to these static problems in section **2**). The dynamics is also very complex : my vision of avalanches is presented in section **3** — but it is probably naive and incomplete.

Not only we do have a great variety of grains : but also a great variety of interactions, commanding the adhesion and the friction between grains. For instance, during dry periods, the grains of sand in a dune have no cohesion, and under the action of wind, the dune moves [2]. In more humid intervals, the grains stick together through minute humidity patches, and they are not entrained by the wind : the dunes stop, thus relieving the plantations from a serious threat. In the present text, we shall concentrate on dry systems, with no cohesion, which give us a relatively well defined model system.

2 Statics

2.1 The general problem

Over more than a hundred years, the static distribution of stresses in a granular sample has been analyzed in departments of Applied Mechanics, Geotechnical Engineering, and Chemical Engineering. What is usually done is to determine the relations between stress and strain on model samples, using the so called triaxial tests. Then, these data are integràted into the problem at hand, with the material divided into finite elements. There is one complication however. To define a strain in a sample, we must know an *unstrained reference state*. This is easily found for a conventional solid, which has a shape. It is less clear for a powder sample : a) the way in which we filled the container for the triaxial test may play a role. b) when we transpose the triaxial data to the field, we are in fact assuming that our field material has had one particular mechanical history.

I tend to believe that, in a number of cases, the problem of the reference state can be simplified, because the sample has not experi-

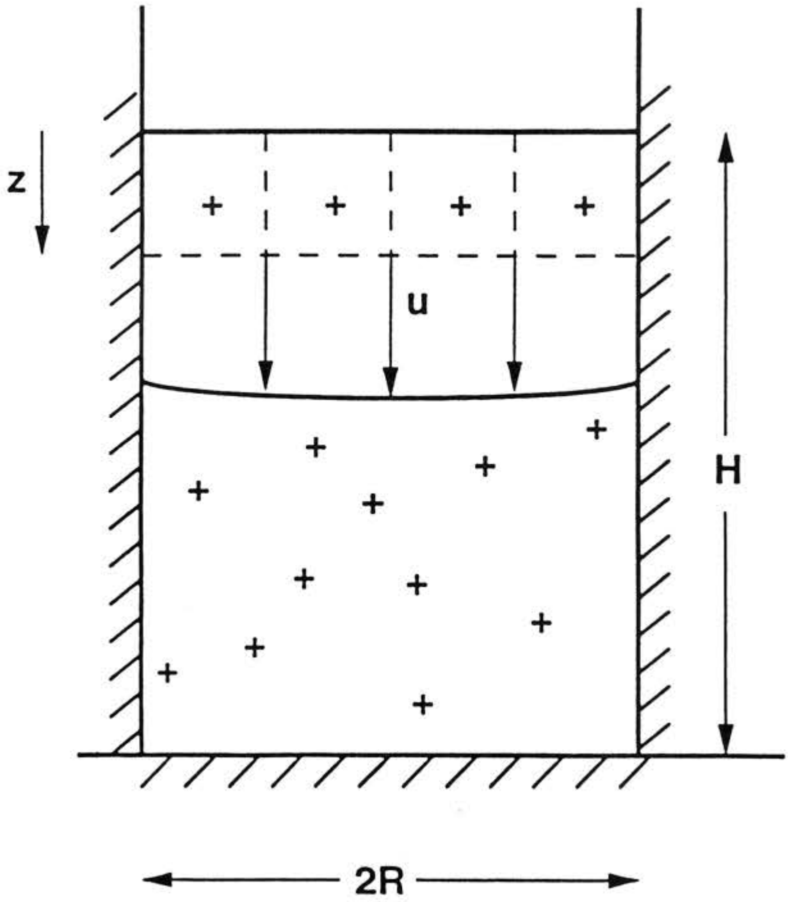

Fig. 1. A silo filled with grains, up to a height H. The grains are assumed to undergo very small vertical displacements u, for which an elastic description makes sense. They rub against the lateral walls.

enced any dangerous stress since the moment, when the grains "froze" together : this leads to a quasi elastic description, which is simple. I will try to make these statements more concrete by choosing one exempla : a silo filled with grain.

2.2 The Janssen picture for a silo

The problem of a *silo* (fig. 1) is relatively simple. The stresses, measured with gauges at the bottom, are generally much smaller than the hydrostatic pressure $\rho g H$ which we would have in a liquid (ρ : density, g : gravitational acceleration, H : column height). A first modelisation for this was given long ago by Janssen [3] and Lord Rayleigh [4].

a) Janssen assumes that the horizontal stresses in the granular medium (σ_{xx}, σ_{yy}) are proportional to the vertical stresses :

$$\sigma_{xx} = \sigma_{yy} = k_j \sigma_{zz} = -k_j p(z) \tag{1}$$

where k_j is a phenomenological coefficient, and $p = -\sigma_{zz}$ is a pressure.

b) An important item is the friction between the grains and the vertical walls. The walls endure a stress σ_{rz}. The equilibrium condition for a horizontal slice of grain (area πR^2, height dz) gives :

$$-\rho g + \frac{\partial p}{\partial z} = \frac{2}{R} \sigma_{rz} \mid_{r=R} \tag{2}$$

(where r is a radical coordinate, and z is measured positive towards the bottom).

Janssen *assumes* that, everywhere on the walls, the friction force has reached its maximum allowed value -given by the celebrated law of L. da Vinci and Amontons [5]:

$$\sigma_{rz} = -\mu_f \sigma_{rr} = -\mu_f k_j p \tag{3}$$

where μ_f is the coefficient of friction between grains and wall.

Accepting eqs (1) and (3), and incorporating them into eq. (2), Janssen arrives at :

$$\frac{\partial p}{\partial z} + \frac{2\mu_f}{R} k_j p = \rho g \tag{4}$$

This introduces a characteristic length :

$$\lambda = \frac{R}{2\mu_f k_j} \tag{5}$$

and leads to pressure profiles of the form :

$$p(z) = p_\infty \left[1 - \exp(-z/\lambda)\right] \tag{6}$$

with $p_\infty = \rho g \lambda$. Near the free surface ($z < \lambda$) the pressure is hydrostatic ($p \sim \rho g z$). But at larger depths ($z > \lambda$)$p \to p_\infty$: all the weight is carried by the walls.

2.3 Critique of the Janssen picture

This Janssen picture is simple, and does give the gross features of stress distributions in silos. But his two assumptions are open to some doubt.

a) If we take an (excellent) book describing the problem as seen from mechanics department [6], we find that relation (1) is criticized : a constitutive relation of this sort might be acceptable if x, y, z were the principal axes of the stress tensor — but in fact, in the Janssen model, we also need non vanishing off diagonal components σ_{xz}, σ_{yz}.

b) For the contact with the wall, it is entirely arbitrary to assume full mobilisation of the friction, as in eq. [3]. In fact, any value σ_{rz}/σ_{rr} below threshold would be acceptable. Some tutorial examples of this condition and of its mechanical consequences are presented in Duran's book [1]. I discussed some related ambiguities in a recent note [7].

2.4 Quasi elastic model

When a granular sample is prepared, we start from grains in motion, and they progressively freeze into some shape : this defines our reference state. For instance, if we fill a silo from the center, we have continuous avalanches running towards the walls, which stop and leave us with a certain slope.

As we shall see in section **3**, this final slope, in a "closed cell" geometry like the silo, is always *below critical* : we do not expect to be close to an instability in shear. In situations like this, we may try to describe the granular medium as a *quasi elastic medium*. The word "quasi" must be explained at this point.

When we have a granular system in a certain state of compaction, it will show a resistance to compression, measured by a macroscopic bulk modulus K. But the forces are mediated by small contact regions between two adjacent grains, and the contact areas increase with pressure. The result is that $K(p)$ increases with p. For spheroidal objects and purely Hertzian contacts, one would expect $K \sim p^{1/3}$, while most experiments are closed to $K \sim p^{1/2}$ [9]. Tentative interpretations of the $p^{1/2}$ law have been proposed [10] [11].

Thus, following [12], we assume now that we can use an elastic description of the material in the silo -since we do not expect any slip band in the silo. To start, we introduce a displacement field $\underset{\sim}{u}(\underset{\sim}{r})$; for instance, with a laboratory column, we would define a reference state with a filled horizontal column, then rotate it to vertical, and measure some very small displacements u of the grains towards the bottom. The only non vanishing component of u is u_z.

We further assume, for the moment, that our medium can be described locally as *isotropic*, with two Lame coefficients, or equivalently a bulk modulus K, plus a shear modulus μ. We can then write the vertical and horizontal constraints in the standard form :

$$\sigma_{zz} = \left(K + \frac{4\mu}{3}\right)\frac{\partial u_z}{\partial z} \tag{7}$$

$$\sigma_{xx} = \sigma_{yy} = \left(K - \frac{2\mu}{3}\right)\frac{\partial u_z}{\partial z} \tag{8}$$

Comparing the two, we do get a Janssen relation, with :

$$k_j = \frac{\sigma_{xx}}{\sigma_{zz}} = \frac{3K - 2\mu}{3K + 4\mu} = \frac{\sigma}{1-\sigma} \tag{9}$$

where σ is the Poisson ratio.

In our picture, K and μ may still be functions of the scalar pressure $-(\sigma_{xx} + \sigma_{yy} + \sigma_{zz})$, or equivalently of $p(z)$. Here we assume, for simplicity, that σ is independent of p. This will have to be checked in the future.

How do we get the stresses σ_{rz}? We have :

$$\sigma_{rr} = 2\mu\frac{\partial u_z}{\partial z} \tag{10}$$

and this imposes :

$$u_z = u_0(z) - \frac{1}{2}C(z)r^2 \tag{11}$$

where u_0 is the value at the center point, and the correction C is obtained by comparison with eq. (2) :

$$\sigma_{rr} = -2\mu Cr = \frac{r}{2}\left(\rho g + \frac{\partial p}{\partial z}\right) \tag{12}$$

giving :

$$C(z) = (4\mu)^{-1}\left[\rho g - \frac{\partial p}{\partial z}\right] \tag{13}$$

The correction $-1/2Cr^2$ in eq. (11) must be compared to u_0.

Taking derivatives, we find :

$$\frac{\frac{\partial}{\partial z}(CR^2)}{\frac{\partial}{\partial z}(u_0)} = R\frac{1}{p}\frac{dp}{dz} \cong \frac{R}{\lambda} \tag{14}$$

thus, the whole description is strictly consistent if $\lambda \gg R$ or $\mu_f \ll 1$.

2.5 State of partial mobilisation

At this stage, we have (to our best) answered the first critique to the Janssen model. Let us now turn to the description of friction. Following ref. [7], we are led to replace the macroscopic threshold law of eq. [3] by a more detailed law, involving the displacement $u_z = u$ near the wall surface. The idea is that, for very small distortions, the friction force is harmonic — proportional to u. But when u is larger than a certain anchoring length Δ, the friction force saturates to the Amontons limit. In ref. [7], I used a specific model of bistable asperities (Caroli Nozières) to substantiate this assumption. But, more general friction systems (involving some plastic deformations at the contact points) are also compatible with this description. Thus, we are led to write :

$$-\sigma_{rz} = \sigma_{rr}\mu_f\psi\left(\frac{u}{\Delta}\right) \tag{15}$$

where $\psi(x)$ is a crossover function with $\psi(x) \sim x$ for $x \to 0$ and $\psi(x) \to 1$ for $|x| \gg 1$.

The few data available on macroscopic friction systems with smooth surfaces suggest $\Delta \sim 1$ micron (comparable to the size of an asperity). For our grains, rubbing against the wall of a silo, Δ is largely unknown. When $|u| < \Delta$, we say that the friction is only *partly mobilised.*

a) Let us assume first that we have *no mobilisation.* Then $p(z)$ is hydrostatic : $p = \rho g z$, and we have a local deformation :

$$\frac{\partial u}{\partial z} = \frac{\rho g z}{\tilde{K}} \tag{16}$$

where $\tilde{K} = K + 4\mu/3$. This is associated with a boundary condition at the bottom of the silo :

$$u(z = H) = 0 \tag{17}$$

The result is a displacement at the free surface :

$$u_s \equiv u(z = 0) = \rho g H^2/(2\,\tilde{K}) \tag{18}$$

Our assumption of weak mobilisation is consistent if $u_s < \Delta$, or equivalently $H < H^*$, where H^* is a critical column height, defined by :

$$H^{*2} = 2\,\tilde{K}\,\Delta/(\rho g) \tag{19}$$

Typical, with $\Delta =$ 1micron, we expect $H^* \sim 30$ cm.

b) What should happen if our column is now higher than H^*? Let us assume now that friction is mobilised in most of the column. If $H > \lambda$, this implies that $p \sim p_\infty$: thus, the deformation must be :

$$\frac{du}{dz} = \frac{p_\infty}{\tilde{K}} \tag{20}$$

Let us investigate the bottom of the silo, putting $z = H - \eta$. At $\eta = 0$, we have $u = 0$. Thus, using eq. (20), we reach :

$$\frac{u}{\Delta} = \frac{\eta p_\infty}{\Delta\,\tilde{K}} = \frac{2\eta\lambda}{H^{*2}} \tag{21}$$

We see that the bottom part is not mobilised ($u < \Delta$) up to a level :

$$\eta = \eta^* \equiv \frac{H^{*2}}{2\lambda} \qquad (H^* < \lambda) \tag{22}$$

Eq. (22) holds only if $p(z)$ is close to p_∞ in the region of interest : this imposes $\eta^* < \lambda$, or equivalently $H^* < \lambda$. In the opposite case, the pressure field $p(z)$, in the interval $0 < \eta < \eta^*$, would again be hydrostatic, with $u \sim \rho g \eta^2 / \widetilde{K}$.

This gives us :

$$\eta^* = H^* \qquad (H^* > \lambda) \tag{23}$$

The Janssen model holds only if $H \gg \eta^*$.

The conclusion (for all values of H^*/λ) is that Janssen can apply only for heights $H \gg H^*$. This is probably satisfied in industrial silos, but not necessarily in laboratory columns. Certain observed disagreements between $p(z)$, measured in columns, and the Janssen model, may reflect this [13].

The authors of ref. [13] have also made an important observation : the temperature cycles between day and night lead to significant modulations of $p(z)$. This, as they point out, must be a dilation effect : the differential dilations experienced by the grains and the wall can easily lead to vertical displacements u which are comparable to the anchoring length : mobilisation may be very different during night and day.

2.6 Stress distribution in a heap

Below a heap of sand, the distribution of normal pressures on the floor is not easy to guess. In some cases, the pressure is not a maximum at the center point ! This has led to a vast number of physical conjectures, describing "arches" in the structure [14] [15] [16]. In their most recent form [16], what is assumed is that, in a heap, the principal axis of the stress are fixed by the deposition procedure. Near the free surface, following Coulomb [6], it is usually assumed that (for a material of zero cohesion) the shear and normal components of the stress (τ and σ_n) are related by the condition :

$$\tau = \sigma_n \mu_i = \sigma_n \tan \theta_{\max} \tag{24}$$

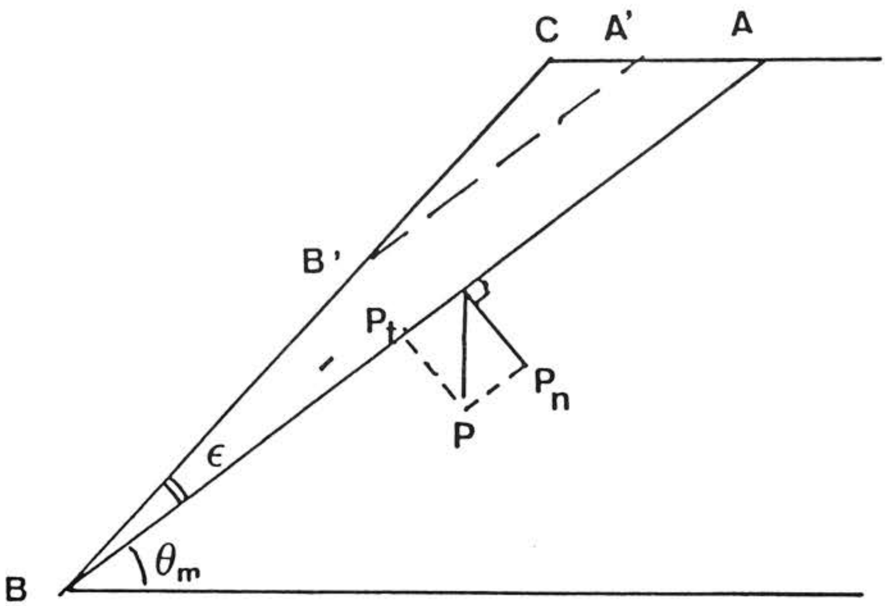

Fig. 2. The Coulomb method of wedges to define the angle $\theta_{\max}$ at which an avalanche starts.

where μ_i is an interval friction coefficient and tan $\theta_{\max}$ is the resulting slope. In a 2 dimensional geometry, this corresponds to a principal axes which is at an angle $2\theta_{\max}$ from the horizontal (fig. 2) [6]. The assumption of ref. [16] is that this orientation is retained in all the left hand side of the heap (plus a mirror symmetry for the right hand side). Once this is accepted, the equilibrium conditions incorporating gravity, naturally lead to a "channeling of forces" along the principal axes, and to a distribution of loads on the bottom which has two peaks This point of view has been challenged by S. Savage [17] who recently gave a detailed review of the experimental and theoretical literature. He makes the following points :

a) for 2 dimensional heaps ("wedges") with a rigid support plane, there is no dip in the experiments.

b) if the support is (very slightly) deformable, the stress field changes deeply, and a dip occurs.

c) for the 3d case ("cones") the results are extremely sensitive to the details of the deposition procedure.

Savage also describes finite element calculations, where one imposes the Mohr Coulomb conditions (to which we come back in section **3**) at the free surface of a wedge. If we had assumed a quasi elastic description inside, we would have found an inconsistency : there is a region, just below the surface, which becomes instable towards shear and slippage. Thus Savage uses Mohr Coulomb in a finite sheet near the surface, plus elastic laws in the inner part : with a rigid support he finds no dip. But, with a deformable support, he gets a dip.

In my opinion, the Savage picture contains the essential ingredients. There may exist an extra simplification, however -which I already announced in connection with the silos. If we look at the formation of the heap (as we shall do in section **3**) we find that the slope angle upon disposition should be *lower* than the critical angle $\theta_{\max}$. Thus our system is prepared in non critical conditions : all the sample may then be described as quasi elastic. This, in fact, should not bring in very great differences from the Savage results.

I suspect that, what the physicists really wanted to incorporate, is the possible importance of an internal *texture* [18]. If we look at the contacts $(1, 2, \cdots, i, \cdots, p)$ of a grain in the structure, we can form two characteristic tensors: one is purely geometrical and defines what I shall call the texture :

$$Q_{\alpha\beta} = \sum_i x_\alpha^{(i)} x_\beta^{(i)} \tag{25}$$

(where x_α are the distances measured from the center of gravity of the grain). The other tensor is the static stress :

$$\sigma_{\alpha\beta} = \frac{1}{2} \sum_i \left(x_\alpha^{(i)} F_\beta^{(i)} + x_\beta^{(i)} F_\alpha^{(i)} \right) \tag{26}$$

where $\underset{\sim}{F}^{(i)}$ is the force transmit ted at contact (i). There is no reason for the axes of these two tensors to coincide. For instance, in an ideal hexagonal crystal, one major axes of the Q tensor is the hexagonal axis, while the stresses can have any set of principal axes. In the heap problem, I am ready to believe that the deposition process freezes a certain structure for the Q tensor, but not for the stress tensor.

The presence of a non trivial Q tensor (or "texture") can modify the quasi elastic model : instead of using an isotropic medium, as was done here in eqs (7, 8) for the silo, we may need an anisotropic medium. In its simplest version, we would assume that the coarse-grained average $Q_{\alpha\beta}$ has two degenerate eigenvalues, and one third eigenvalue, along a certain unit vector (the director) $\underset{\sim}{n}(\underset{\sim}{r})$. Thus, a complete discussion of static problems, in the absence of strong shear bands, would involve an extra field $\underset{\sim}{n}$ defined by the construction of the sample. But this refinement is, in a certain sense, minor. Texture effects should not alter deeply the quasi elastic picture.

3 Dynamics : avalanche problems

3.1 Onset and evolution of surface flows

3.1.1 The Coulomb view

As already mentioned in section **2**, C.A. Coulomb (who was at the time a military engineer) noticed that a granular system, with a slope angle θ, larger than a critical value $\theta_{\max}$, would be unstable. He related the angle $\theta_{\max}$ to the friction properties of the material. For granular materials, with negligible adhesive forces, this leads to $tg\theta_{\max} = \mu_i$, where μ_i is a friction coefficient [6]. The instability generates an avalanche. What we need is a detailed scenario for the avalanche.

We note first that the Coulomb argument is not complete : a) it does not tell us at what angle $\theta_{\max} + \varepsilon$ the process will actually start b) it does not tell us which gliding plane is prefered among all these of angle $\theta_{\max}$) as shown on fig.2.

I shall propose an answer to these questions based on the notion of a characteristic size ξ in the granular material.

1) Simulations [19] [20] and experiments [21] indicates that the forces are not uniform in a granular medium, but that there are force paths conveying a large fraction of the force. These paths have a certain mesh size ξ, which is dependent on the grain shapes, on the friction forces between them, etc, but which is typically $\xi \sim 5$ to 10 gram diameters d.

2) We also know that, under strong shear, a granular material can display *slip bands* [22]. The detailed geometry of these bands depends on the imposed boundary conditions. But the minimum thickness of a slip band appears to be larger than d. We postulate that the minimum size *coincides with the mesh size* ξ.

We are then able to make a plausible prediction for the onset of the Coulomb process : the thickness of the excess layer must be of

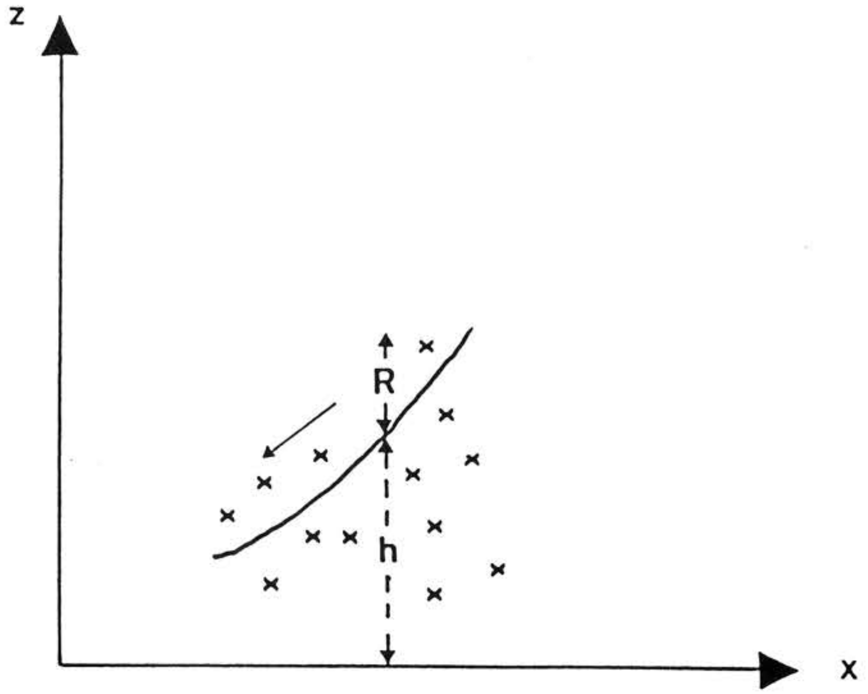

Fig. 3. The basic assumption of the BCRE picture is that there is a sharp distinction between immobile grains with a profile $h(x,t)$ and rolling grains of density $R(x,t).R$ is measured in units of "equivalent height" : collision processes conserve the sum $h+R$.

order ξ ; and the excess angle ε must be of order ξ/L, where L is the size of the free surface.

Thus, at the moment of onset, our picture is that a layer of thickness $\sim \xi$ starts to slip. It shall then undergo various processes : (i) the number of grains involved shall be fluidized by the collisions on the underlying heap (ii) it shall be amplified because the rolling grains destabilize some other grains below. The steady state flow has been studied in detailed simulations [23]. It shows a sharp boundary between rolling grains and immobile grains : this observation is the starting point of most current theories.

The amplification process was considered in some detail by Bouchaud et al. in a classic paper of 1994 (refered to here at BCRE [24] [25]. It is important to realise that, if we start an avalanche with a thickness ξ of rolling species, we rapidly reach much larger thicknesses R : in practice, with macroscopic samples, we deal with *thick avalanches* ($R \gg \xi$). We are mainly interested in these regimes — which, in fact, turn out to be relatively simple

3.1.2 Modified BCRE equations [26]

BCRE discuss surface flow on a slope of profile $h(x,t)$ and slope $tg\theta \cong \theta = \partial h/\partial x$,with a certain amount $R(x,t)$ of rolling species (fig. 3). In ref. [24], the rate equation for the profile is written in the form :

$$\frac{\partial h}{\partial t} = \gamma R(\theta_n - \theta) \qquad (+\text{diffusionterms}) \tag{27}$$

This gives erosion for $\theta > \theta_n$, and accretion for $\theta < \theta_n$.

We call θ_n the neutral angle. This notation differs from BCRE who called it θ_r(the angle of repose). Our point is that different experiments can lead to different angles or repose, not always egal to θ_n.

For the rolling species, BCRE write :

$$\frac{\partial R}{\partial t} = -\frac{\partial h}{\partial t} + v\frac{\partial R}{\partial x} \qquad (+\text{diffusionterms}) \tag{28}$$

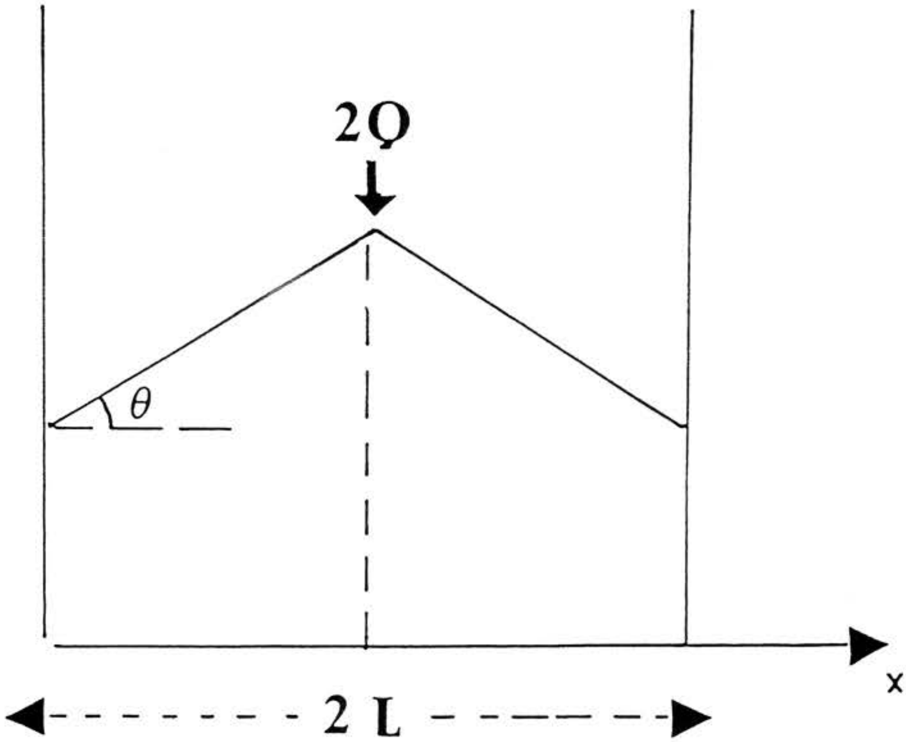

Fig. 4. Feeding of a two dimensional silo with a flux Q over a length L, leading to a growth velocity $w(z) = Q/L$.

where γ is a characteristic frequency, and v a flow velocity, assumed to be non vanishing (and approximately constant) for $\theta \sim \theta_n$. For simple grain shapes (spheroidal) and average levels of inelastic collisions, we expect $v \sim \gamma d \sim (gd)^{1/2}$, where d is the grain diameter and g the gravitational acceleration. Eq. (28) gives $\partial h/\partial t$ as linear in R : this should hold at small R, when the rolling grains act independently. But, when $R > d$, this is not acceptable. Consider for instance the "uphill waves" mentioned by BCRE, where R is constant : eq. (27) shows that an accident in slope moves upward, with a velocity $v_{up} = \gamma R$. It is not natural to assume that v_{up} can become very large for large R.

This lead us (namely T. Boutreux, E. Raphaël, and myself) [26] to propose a modified version of BCRE, valid for flows which involve large R values, and of the form :

$$\frac{\partial h}{\partial t} = v_{up}(\theta_n - \theta) \qquad (R > \xi) \tag{29}$$

where v_{up} is a constant, comparable to v. We shall not see the consequences of this modification.

Remark : in the present problems, the diffusion terms in eq. (28) turn out to be small, when compared to the convective terms (of order d/l, where L is the size of the sample) : we omit them systematically.

3.1.3 A simple case

A simple basic example (fig. 4) is a two dimensional silo, fed from a point at the top, with a rate $2Q$, and extending over a horizontal span $2L$: the height profile moves upward with a constant velocity Q/L. The profiles were already analysed within the BCRE equations (25). With the modified version, the R profile stays the same, vanishing at the wall ($x = 0$) :

$$R = \frac{x}{L}\frac{Q}{v} \tag{30}$$

but the angle is modified and *differs from the neutral angle* : setting $\partial h/\partial t = Q/L$, we arrive at :

$$\theta_n - \theta = \frac{Q}{Lv_{up}} \qquad (Q > v\xi) \tag{31}$$

Thus, we expect a slope which is now dependent on the rate of filling : this might be tested in experiments or in simulations.

3.2 Downhill and uphill motions

Our starting point is a supercritical slope, extending over a horizontal span L with an angle $\theta = \theta_{\max} + \epsilon$ (fig. 2). Following the ideas of section **1**, the excess angle ϵ si taken to be small (of order ξ/L). It will turn out that the exact values of ϵ is not important : as soon as the avalanche starts, the population of rolling species grows rapidly and becomes independent of ϵ (for ϵ small) : this means that our scenarios have a certain level of universality. The crucial feature is that grains roll down, but profiles move uphill : we shall explain this in detail in the next paragraph.

3.2.1 Wave equations and boundary conditions

It is convenient to introduce a reduced profile :

$$\tilde{h}\,(x,t) = h - \theta_n x \tag{32}$$

Following BCRE, we constantly assume that the angles θ are not very large, and write $tg\theta \sim \theta$: this simplifies the notation. Ultimately, we may write eqs (28) and (29) in the following compact form :

$$\frac{\partial R}{\partial t} = v_{up}\frac{\partial \tilde{h}}{\partial x} + v\frac{\partial R}{\partial x} \tag{33}$$

$$\frac{\partial \tilde{h}}{\partial t} = -v_{up} \frac{\partial \tilde{h}}{\partial x} \tag{34}$$

Another important condition is that we must have $R > 0$. If we reach $R = 0$ in a certain interval of x, this means that the system is locally frozen, and we must then impose :

$$\frac{\partial \tilde{h}}{\partial t} = 0 \tag{35}$$

One central feature of the modified eqs (33, 34) is that, whenever $R > 0$, they are linear. The reduce profile $\tilde{h}$ is decoupled from R, and follows a very simple wave equation :

$$\tilde{h}\,(x,t) = v(x - v_{up}t) \tag{36}$$

where w is an arbitrary function describing uphill waves.

It is also possible to find a linear combination of $R(x,t)$ and $\tilde{h}\,(x,t)$ which moves downhill. Let us put :

$$R(x,t) + \lambda\,\tilde{h}\,(x,t) = u(x,t) \tag{37}$$

where λ is an unknown constant. Inserting eq. (37) into eq. (33), we arrive at :

$$\frac{\partial u}{\partial t} - v\frac{\partial u}{\partial x} = [v_{up} - \lambda(v_{up} + v)]\,\frac{\partial \tilde{h}}{\partial x} \tag{38}$$

Thus, if we choose :

$$\lambda = \frac{v_{up}}{v + v_{up}} \tag{39}$$

we find that u is ruled by a simple wave equation, and we may set :

$$u(x,t) = u(x + vt) \tag{40}$$

We can rewrite eq. (37) in the form :

$$R(x,t) = u(x+vt) - \lambda\ w(x - v_{up}t) \tag{41}$$

Eqs (36) and (41) represent the normal solution of our problem in all regions where $R > 0$. This formal solution leads in fact to a great variety of avalanche regimes.

3.2.2 Comparison of uphill and downhill velocities

Our equations introduce two velocities : one downhill (v) and one uphill (v_{up}). How are they related ? The answer clearly depends on the precise shape (and surface features) of the grains. Again, if we go to spheroidal grains and average levels of inelasticity, we may try to relate v_{up} and v by a naive scaling argument. Returning to eq. (27) and (29) for the rate of exchange between fixed and rolling species, we may interpolate between the two limits ($R < \xi$ and $R > \xi$) :

$$\frac{\partial h}{\partial t} = \gamma\xi(\theta - \theta_n) f\left(\frac{R}{\xi}\right) \tag{42}$$

where the unknown function f has the limiting behaviours :

$$\left.\begin{array}{l} f(x \to 0) = x \\ f(\gg 1) = f_\infty = cons\tan t \end{array}\right\} \tag{43}$$

This corresponds to $v_{up} = f_\infty \gamma \xi$. Since we have assumed $v \sim \gamma d$,we are led to :

$$v_{up}/v \sim f_\infty \xi / d \tag{44}$$

If, even more boldly, we assume that $f_\infty \sim 1$, and since ξ is somewhat larger than the grain size, we are led to suspect that v_{up} may be larger than v.

3.2.3 Closed versus open systems

Various types of boundary conditions can be found for our problems of avalanches :

a) At the top of the heap, we may have a situation of zero feeding (R =0). But we can also have a constant injection rate Q fixing $R = Q/v$. This occurs in the silo of fig. 4. It also occurs at the top of a dune under a steady wind, where saltation takes place on the windward side (2), imposing a certain injection rate Q, which then induces a steady state flow on the steeper, leeward side.

b) At the bottom end, we sometimes face a solid wall — e.g. in the silo ; then we talk about a *closed* cell, and impose $R = 0$ at the wall. But in certain experiments, with a rotating bucket, the bottom end is open (fig.5). Here, the natural boundary condition is h = constant at the bottom point, and R is not fixed. Both cases are discussed in ref. [26]. Here, we shall simply describe some features for the closed cell system.

3.3 Scenario for a closed cell

The successive "acts" in the play can be deduced from the wave equations (40, 41) plus initial conditions. Results are shown in figs (6-10). During act **1**, a rolling wave starts from the top, and an uphill wave starts from the bottom end. In act **2**, these waves have passed each other. In act **3**, one of the waves hits the border. If $v_+ > v$, this occurs at the top. From this moment, a region near the top gets frozen, and increases in size. If $v_+ < v$, this occurs at the bottom : the frozen region starts there and expends upwards. In both cases, the final slope θ_f is not equal to the neutral angle θ_n, but is *smaller* : $\theta_f = \theta_n - \delta = \theta_{\max} - 2\delta$.

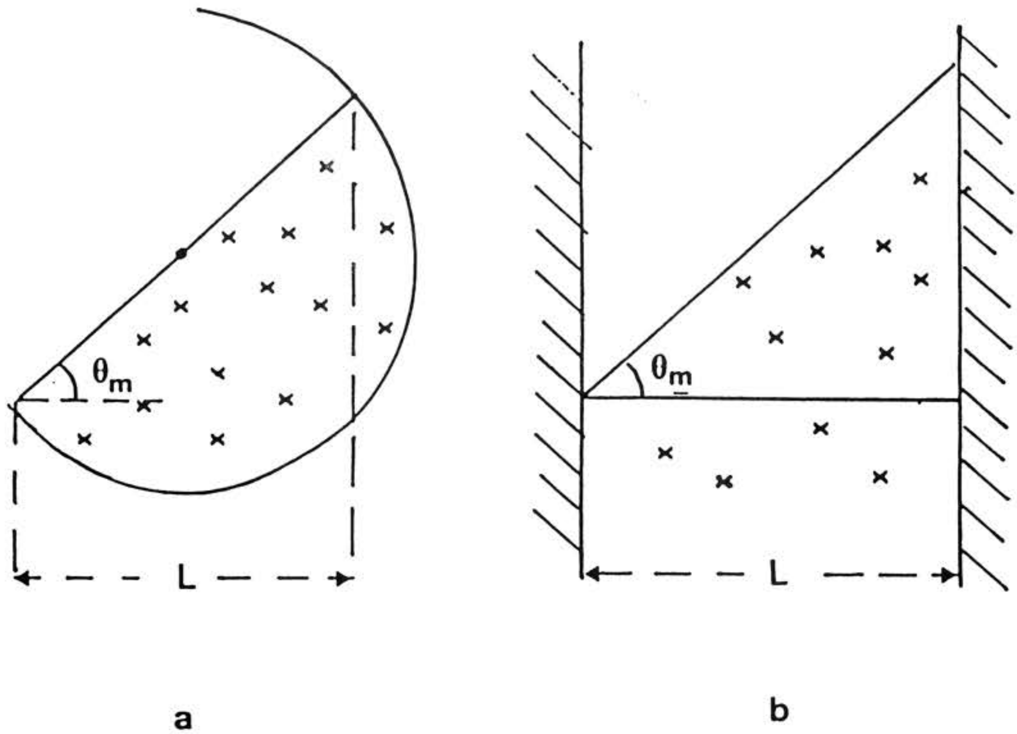

Fig. 5. Two types of avalanches : a) open cell b) closed cell.

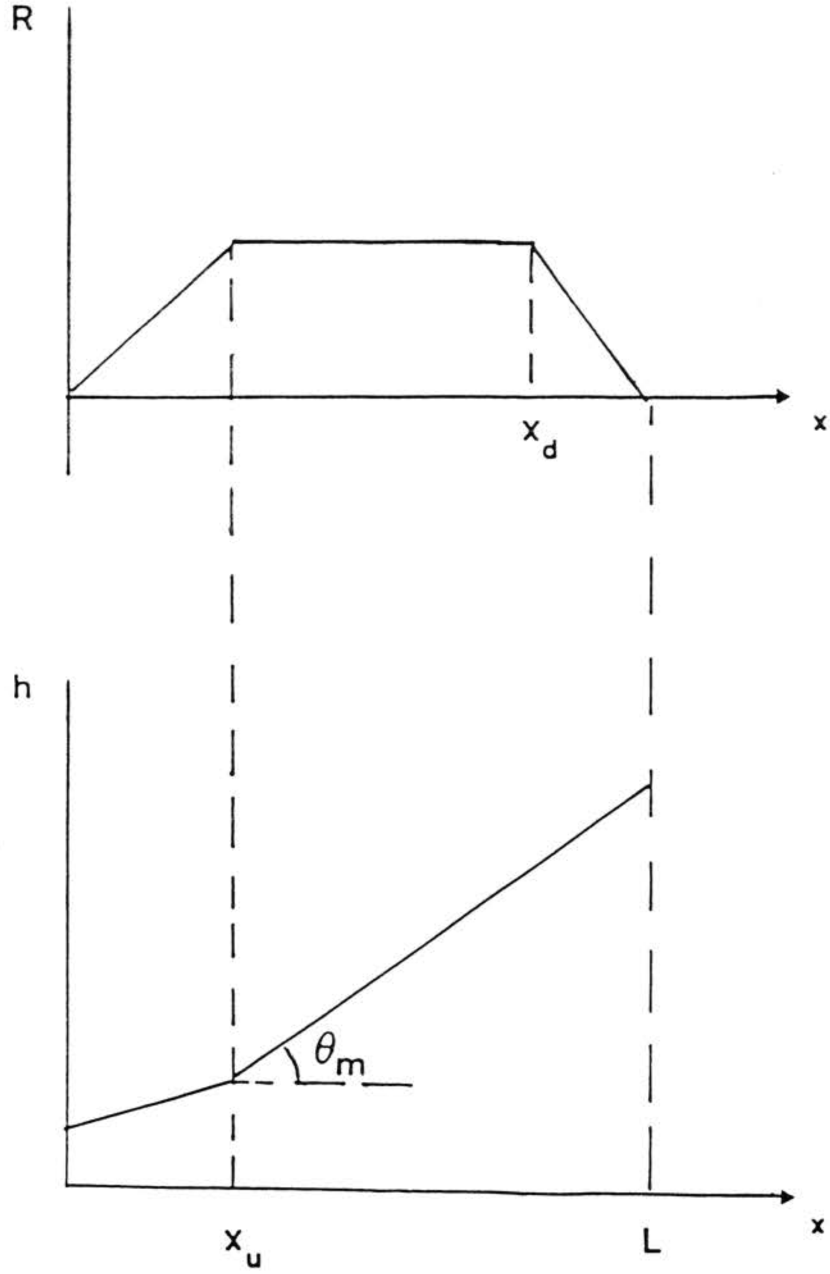

Fig. 6. Closed cell "act **1**". The slope in the bottom region is described by eq. (40).

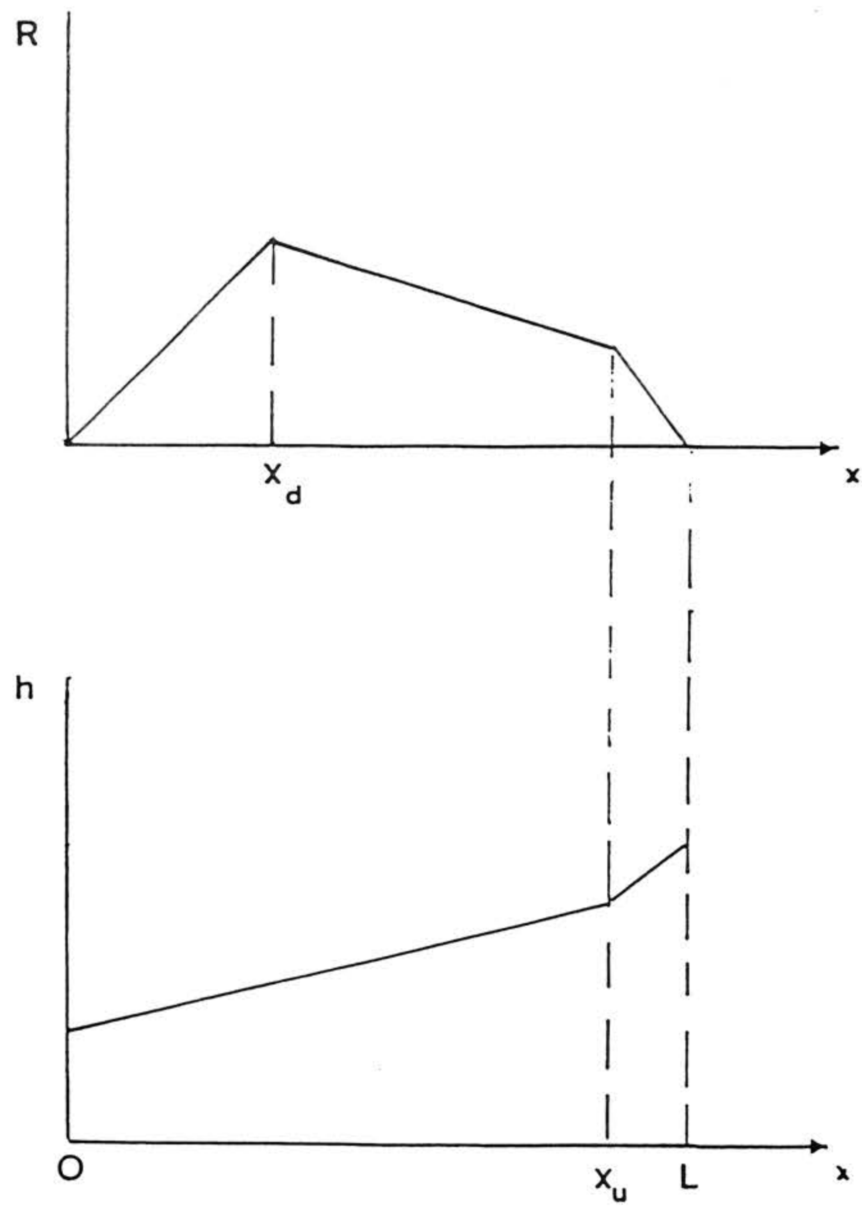

Fig. 7. Closed cell "act **2**". The sketch has been drawn for $v_{up} > v$. (When $v_{up} < v$,the slope $\partial R/\partial x$ in the central region becomes positive).

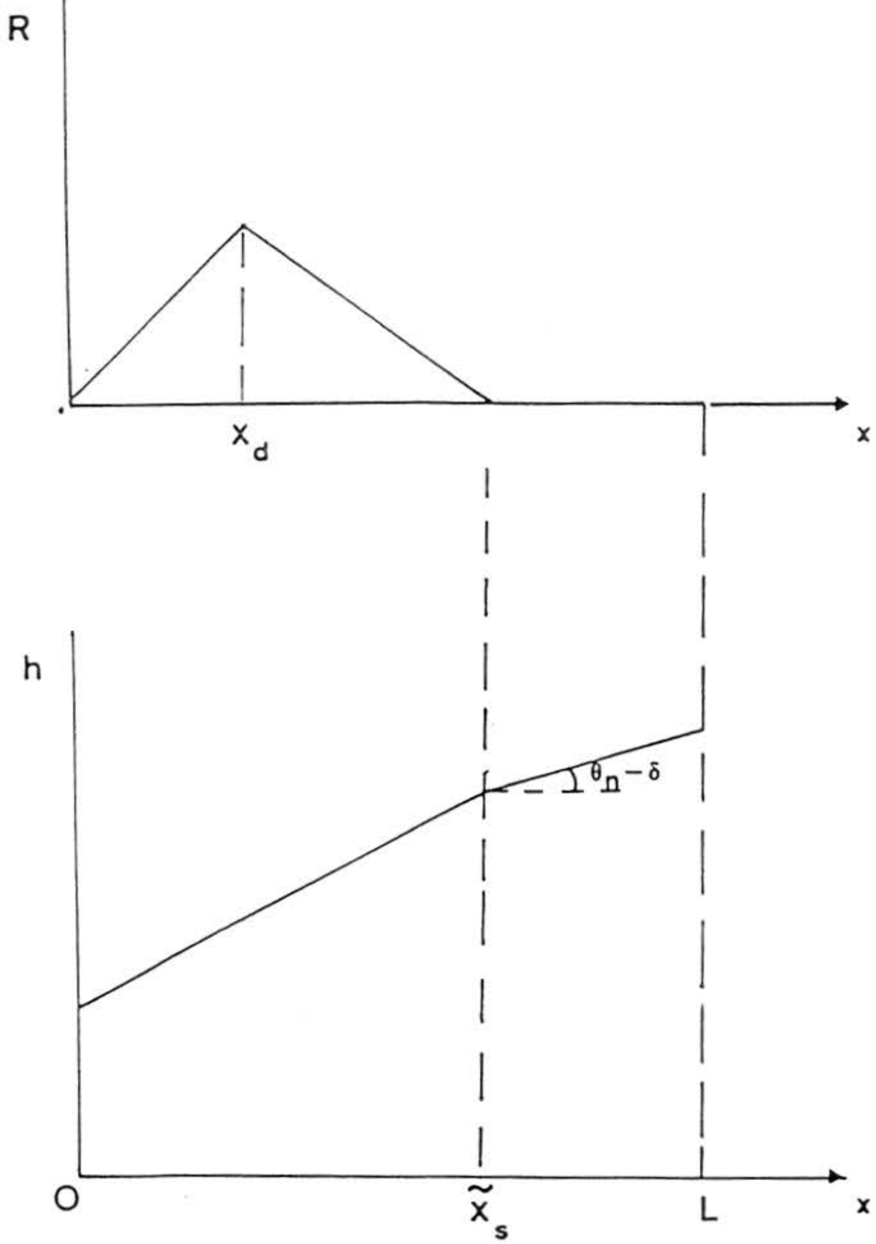

Fig. 8. Closed cell "act **3**". The case $v_{up} > v$. A frozen patch grows from the top.

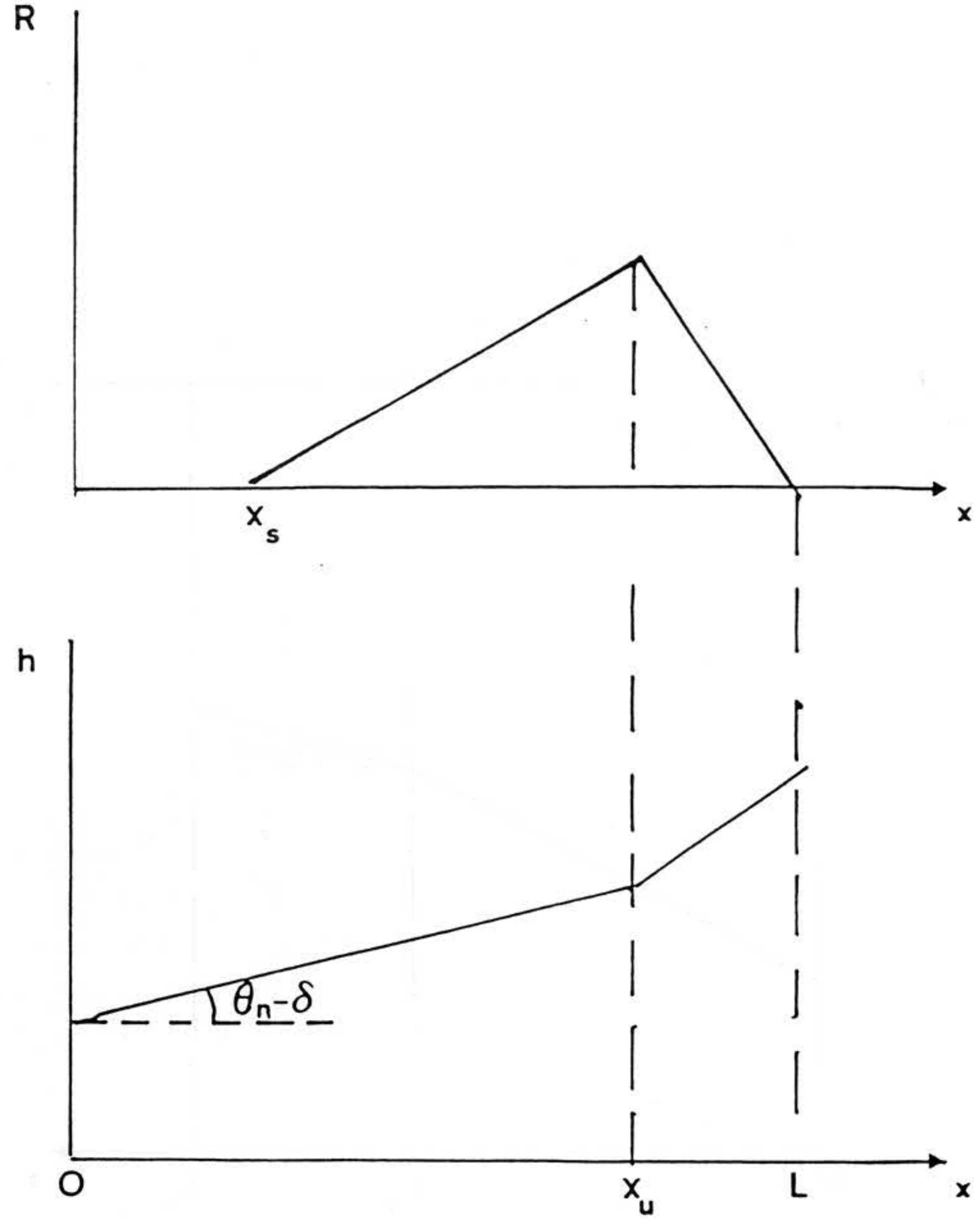

Fig. 9. Closed cell "act **3**" ($v_{up} < v$). Here a frozen patch grows from the bottom

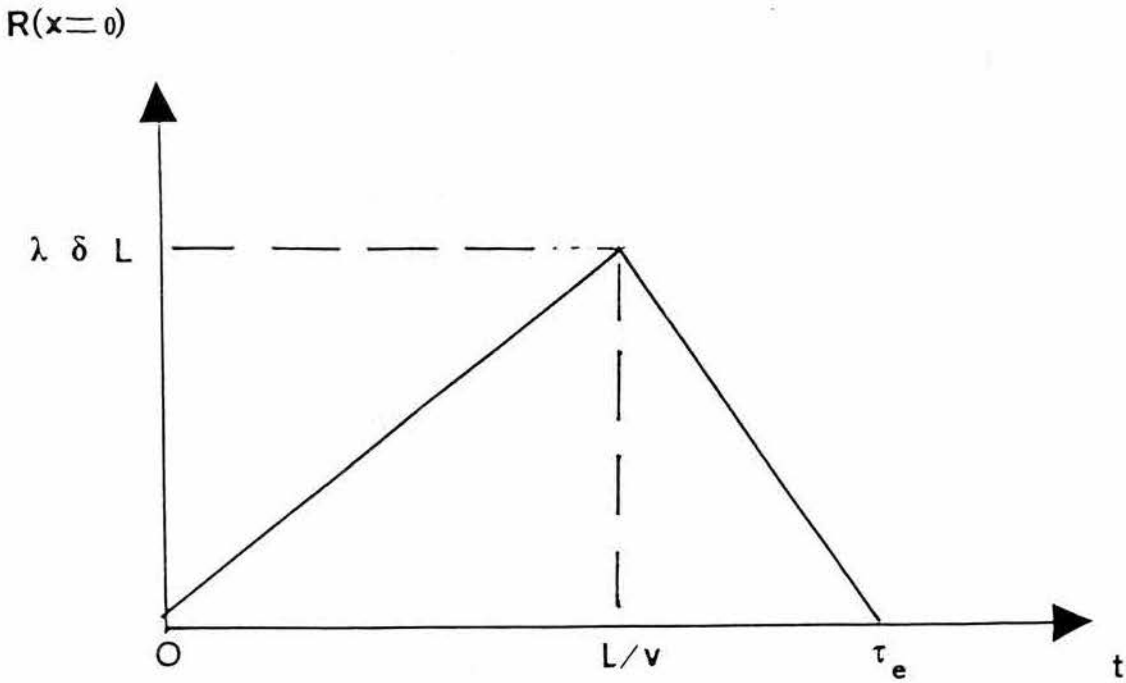

Fig. 10. Flux profile predicted at the bottom of an open cell.

3.4 Discussion

1) The determination of the whole profiles $h(x,t)$ on an avalanche represents a rather complex experiment [27]. But certain simple checks could easily be performed.

a) *With an open cell,* the loss of material measured by $R(0,t)$ is easily obtained, for instance, by capacitance measurement (28). The predictions of ref. [26] for this loss are described on fig. (10). $R(0,t)$ rises linearly up to a maximum at $t = L/v$, and then decreases, reaching 0 at the final time $L(1/v + 1/v_{up})$. The integrated amount is :

$$M \equiv \int R(0,t)dt = \frac{1}{2}\lambda\delta L^2 \left(\frac{2}{v} + \frac{1}{v_{up}}\right) \tag{45}$$

Unfortunately, the attention in ref. [28] was focused mainly on the reproducibility of M, but (apparently) the value of M and the shape of $R(0,t)$ were not analysed in detail.

b) *With a closed cell,* a simple observable is the rise of the height at the bottom $h(0,t)$: this is predicted to increase linearly with time :

$$h(0,t) = \tilde{h}\,(0,t) = \delta v_+ t \tag{46}$$

up to $t = L/v_+$, and to remain constant after.

Similar measurements (both for open or closed cells) could be done at the top point, giving $h(L,t)$.

c) A crucial parameter is the final angle θ_f. In our model, this angle is the same all along the slope. For an open cell, it is equal to the neutral angle θ_n. For a closed cell, it is *smaller* : $\theta_f = \theta_n - \delta$.

Thus the notion of an angle of repose is not universal ! The result $\theta_f = \theta_n - \delta$ was already predicted in a note [28], where we proposed a qualitative discussion of thick avalanches. The dynamics (based on a simplified version of BCRE eqs) was unrealistic — too fast — but the conclusion on θ_f was obvious : in a closed cell, the material which starts at the top, has to be stored at the bottom part, and this leads to a decrease in slope.

d) One major unknown of our discussion is the ratio v_{up}/v. We already pointed out that this may differ for different types of grains. Qualitative observations on a closed cell would be very useful here : if in its late stages (act **3**) the avalanche first freezes at the top, this means $v_{up} > v$. If it freezes from the bottom, v_{up} must be $< v$.

2) Limitations of the present model :

a) Our description is *deterministic* : the avalanche starts automatically at $\theta = \theta_{\max}$, and sweeps the whole surface. In the open cell systems (with slowly rotating drums) one does find a nearly periodic set of avalanche spikes, suggesting that $\theta_{\max}$ is well defined. But the amplitude (and the duration) of these spikes varies [28] : it may be that some avalanches do not start from the top. We can only pretend to represent the full avalanches.

What is the reason for these statistical features ? (i) Disparity in grain size tends to generate spatial in inhomogeneities after a certain number of runs (in the simplest cases, the large grains roll further down and accumulate near the walls). (ii) Cohesive forces may be present : they tend to deform the final profiles, with a $\theta(x)$ which is not constant in space. (iii) Parameters like θ_m (or θ_n) may depend on sample history.

b) *Regions of small R.* For instance, in a closed cell, $R(x,t) \to 0$ for $x \to 0$. A complete solution in the vicinity of $R = 0$ requires more complex equations, interpolating between BCRE and our linear set of equations, as sketched in eq. (42). Boutreux and Raphaël have indeed investigated this point. It does not seem to alter significantly the macroscopic results described here.

c) *Ambiguities in* θ_n. When comparing thick and thin avalanches, we assumed that θ_n is the same for both : but there may, in fact, be a small difference between the two. Since most practical situations are related to thick avalanches, we tend to focus our attention on the "thick" case — but this possible distinction between thick and thin should be kept in mind.

Acknowledgments : I have greatly benefited from discussions and written exchanges with J.P. Bouchaud, J. Duran, P. Evesque, H. Herrmann, and J. Reichenbach.

References

[1] For a general introduction to granular materials, see J. Duran "Poudres et grains" (Eyrolles, Paris 1996).

[2] The basic book here is "Physics of blown sand and sand dunes" by E.R. Bagnold (Chapman and Hall, London 1941).

[3] H.A. Janssen, Z. Vereins Deutsch Eng. 39 (35), p. 1045 (1895).

[4] Lord Rayleigh, Phil Mag 36, 11, 61, 129, 206 (1906).

[5] See for instance "Friction : an introduction", P. Bowden and D. Tabor (Doubleday, NY 1973).

[6] R. Nedermann, "Statics and kinematics of granular materials", Cambridge U. Press, 1992.

[7] P.G. de Gennes, C.R. Acad. Sci. (Paris), (1997).

[8] P. Evesque, J. Physique I (France), 7, p. 1501 (1997).

[9] J. Duffy, R. Mindlin, J. App. Mech. (ASME), 24, p. 585 (1957).

[10] J. Goddard, Proc. Roy. Soc. (London), 430, p. 105 (1990).

[11] P.G. de Gennes, Europhys. Lett., 35, p. 145-149 (1996).

[12] P. Evesque, P.G. de Gennes, submitted to C.R. Acad. Sci. (Paris).

[13] L. Vanel, E. Clément, J. Lanuza, J. Duran, to be published.

[14] S.F. Edwards, C.C. Mounfield, Physica, A 226, p. 1, 12, 25 (1996).

[15] J.P. Bouchaud, M. Cates, P. Claudin, J. Physique II (France), p. 639 (1995).

[16] J.P. Wittmer, M. Cates, P. Claudin, J. Physique I (France), 7, p. 39 (1997).

[17] S.B. Savage, in "Powders and grains" (Behringer and Jenkins, eds), p. 185 (Balkema, Rotterdam) (1997).

[18] H. Herrmann, "On the shape of a sand pile", Proceedings of the Cargèse Workshop (1997), to be published.

[19] F. Radjai et al, Phys. Rev. Lett., 77, p. 274 (1996).

[20] F. Radjain D. Wolf, S. Roux, M. Jean, J.J. Moreau, "Powders and grains" (R. Behringer, J. Jenkins eds), p. 211, Balkema, Rotterdam (1997).

[21] C.H. Liu, S. Nagel, D. Shechter, S. Coppermisth, S. Majumdar, O. Narayan, T. Witten, Science, 269, p. 513 (1995).

[22] J. Desrues, in "Physics of Granular Media" (D. Bideau, J. Dodds eds), p. 127 (Nova Sci. Pub., Les Houches Series (1991).

[23] P.A. Thompson, G.S. Grest, Phys. Rev. Lett., 67, p. 1751 (1991).

[24] –J.P. Bouchaud, M. Cates, R. Prakash, S.F. Edwards, J. Phys. (France), 4, p. 1383 (1994).

–J.P. Bouchaud, M. Cates, in "Dry granular matter", Proceedings of the Cargèse workshop, (1997), H. Hermann ed. (to be published).

[25] P.G. de Gennes, in "Powders and grains" (R. Behringer, J. Jenkins eds), p. 3, Balkema, Rotterdam (1997).

[26] T. Boutreux, E. Raphaël, P.G. de Gennes, to be published.

[27] H. Jaeger, C. Liu, S. Nagel, Phys. Rev. Lett., 62, p. 40 (1988).

[28] T.Boutreux, P.G. de Gennes, C.R. Acad. Sci. (Paris), 324, p. 85-89 (1997).